Acta Societatis Botanicorum Poloniae

DOI: 10.5586/asbp.3604

Publication history
Received: 2018-10-04
Accepted: 2018-11-26
Published: 2018-12-31

Handling editor
Michał Ronikier, W. Szafer Institute of Botany, Polish Academy of Sciences, Poland

Authors' contributions
BZ, HT, ZB, JWB, and AK conceived and designed the experiments and performed the field measurements (BZ: spectrometric measurements; HT, ZB, JWB: plant traits); MK and BZ conducted statistical analyses; all authors wrote the paper

Funding
Research has been carried out under the Polish-Norwegian Research Program of the Polish National Center for Research and Development (NCBiR), project: "Ecosystem stress from the combined effects of winter climate change and air pollution – how do the impacts differ between biomes? (WICLAP)", No: POL-NOR/198571/83/2013, and from the Svalbard Environmental Protection Fund (project 17/37) to JWB and HT. The publishing costs were financed from the theme No. 501-D119-64-0180200-15 awarded by the Polish Ministry of Science and Higher Education.

Competing interests
BW served as guest editor of the issue; other authors: no competing interests have been declared

Citation
Zagajewski B, Kycko M, Tømmervik H, Bochenek Z, Wojtuń B, Bjerke JW, et al. Feasibility of hyperspectral vegetation indices for the detection of chlorophyll concentration in three high Arctic plants: *Salix polaris*, *Bistorta vivipara*, and *Dryas octopetala*. Acta Soc Bot Pol. 2018;87(4):3604. https://doi.

ORIGINAL RESEARCH PAPER

Feasibility of hyperspectral vegetation indices for the detection of chlorophyll concentration in three high Arctic plants: *Salix polaris*, *Bistorta vivipara*, and *Dryas octopetala*

Bogdan Zagajewski[1]*, Marlena Kycko[1], Hans Tømmervik[2], Zbigniew Bochenek[3], Bronisław Wojtuń[4], Jarle W. Bjerke[2], Andrzej Kłos[5]

[1] Department of Geoinformatics, Cartography and Remote Sensing, Faculty of Geography and Regional Studies, University of Warsaw, Krakowskie Przedmieście 30, 00-927 Warsaw, Poland
[2] FRAM – High North Research Center for Climate and the Environment, Norwegian Institute for Nature Research (NINA), PO Box 6606 Langnes, 9296 Tromsø, Norway
[3] Institute of Geodesy and Cartography (IGiK), Zygmunta Modzelewskiego 27, 02-679 Warsaw, Poland
[4] Department of Ecology, Biogeochemistry and Environmental Protection, Faculty of Biological Sciences, University of Wrocław, Kanonia 6/8, 50-328, Wrocław, Poland
[5] Independent Department of Biotechnology and Molecular Biology, University of Opole, Kard. B. Kominka 6, 45-032 Opole, Poland

* Corresponding author. Email: bogdan@uw.edu.pl

Abstract
Remote sensing, which is based on a reflected electromagnetic spectrum, offers a wide range of research methods. It allows for the identification of plant properties, e.g., chlorophyll, but a registered signal not only comes from green parts but also from dry shoots, soil, and other objects located next to the plants. It is, thus, important to identify the most applicable remote-acquired indices for chlorophyll detection in polar regions, which play a primary role in global monitoring systems but consist of areas with high and low accessibility. This study focuses on an analysis of in situ-acquired hyperspectral properties, which was verified by simultaneously measuring the chlorophyll concentration in three representative arctic plant species, i.e., the prostrate deciduous shrub *Salix polaris*, the herb *Bistorta vivipara*, and the prostrate semievergreen shrub *Dryas octopetala*. This study was conducted at the high Arctic archipelago of Svalbard, Norway. Of the 23 analyzed candidate vegetation and chlorophyll indices, the following showed the best statistical correlations with the optical measurements of chlorophyll concentration: Vogelmann red edge index 1, 2, 3 (VOG 1, 2, 3), Zarco-Tejada and Miller index (ZMI), modified normalized difference vegetation index 705 (mNDVI 705), modified normalized difference index (mND), red edge normalized difference vegetation index (NDVI 705), and Gitelson and Merzlyak index 2 (GM 2). An assessment of the results from this analysis indicates that *S. polaris* and *B. vivipara* were in good health, while the health status of *D. octopetala* was reduced. This is consistent with other studies from the same area. There were also differences between study sites, probably as a result of local variation in environmental conditions. All these indices may be extracted from future satellite missions like EnMAP (Environmental Mapping and Analysis Program) and FLEX (Fluorescence Explorer), thus, enabling the efficient monitoring of vegetation condition in vast and inaccessible polar areas.

Keywords
Arctic plants; ASD FieldSpec; remote sensing indices; remote sensing

org/10.5586/asbp.3604

Introduction

Imaging spectroscopy, which consists of recording electromagnetic radiation in hundreds of narrow bands (2–5 nm), makes it possible to analyze how electromagnetic radiation interacts with the analyzed matter [1]. The selective absorption, reflection, or transmission of various wavelengths allows a detailed analysis of the spectral properties of individual plants and vegetation communities [2]. Spectrometer measurements are carried out in both the visible range (VIS, 400–700 nm), near infrared range (NIR, 700–1,500 nm), short-wave infrared range (SWIR, 1,500–2,500 nm), thermal infrared range (TIR, 8,000–15,000 nm), and finally in the microwave range (1 cm–1 m) [3]. A basic measure is spectral reflectance, which indicates the quotient of energy reflected from the incident energy of a given electromagnetic spectrum [4]. Spectral properties of plants depend on their anatomical structure, morphology, and physiological processes [5]. Visible radiation that reaches the plant is absorbed and reflected. The absorbed radiation is used in photosynthesis and fluorescence processes and is emitted as heat. Chlorophyll, carotenoids, and anthocyanins absorb photons of light in the visible range. In infrared, reflection depends on the plant's cellular structures [6], its water concentration [7], its chemical components [8], leaf thickness [9], roughness of leaf surface and canopy [10], the physiological age and arrangement of leaves [11], habitat exposure, solar radiation, phonological period, and various types of diseases and vegetation damage [12]. VIS and NIR wavelengths play an important role in the identification of pigments, e.g., chlorophylls, xanthophylls, and carotenoids. Spectral characteristics (reflectance in selected wavelengths) are used to calculate remote sensing vegetation indices [12], which use various mathematical combinations of relevant coefficients to identify the analyzed properties of plants. Vegetation indices can be divided into many groups and can be used to conduct assessments of different vegetation features, e.g., its general condition, the concentration of photosynthetically active pigments, the amount of light used in photosynthesis, levels of nitrogen in the plants, dry biomass, organic carbon, and water content. Quantitative measurements of chlorophyll, the main photosynthetically active pigment, and protective pigments allow for the assessment of plant condition and potential different stress factors [13]. An analysis performed by Gitelson [14] demonstrates that the relationship between the chlorophyll concentration and the amount of accumulated light is nonlinear, as the absorption per unit of chlorophyll decreases at high chlorophyll concentrations [14]. Some plants can modulate light absorption during the process of photosynthesis through the use of mechanisms such as leaf movement, leaf angle adjustments [15], covering the leaves with substances such as wax [16], and changing the concentration of certain pigments, e.g., anthocyanin [17]. Photochemical processes use most of the energy absorbed by chlorophyll [18]. Some of the energy that reaches the plants is used to produce sugars. The rest is lost in the form of heat or re-emitted as fluorescence. These processes complement each other, and the level of each of them depends on the levels of the other two [19].

Chlorophylls are responsible for about 65% of the photosynthesis process, while the share of carotenoids (with xanthophylls) is approximately 35%; although these proportions vary depending on the phenological period of the analyzed plant species [20,21]. The ratio of chlorophylls to carotenoids is an indicator of plant health and constitutes a characteristic value for individual species [22]. High concentrations of chlorophyll are characteristic of plants in good condition, which translates into high reflectance in the green range of the electromagnetic spectrum and absorption in the blue and red ranges [23]. Quantitative studies of vegetation are related to plant indices [24]; they require calibration with biophysical variables [25]. Currently, they are used to assess crops, e.g., soil property modeling [26,27], irrigation efficiency [28], adaptation to stress factors [29], and the identification of dominant types of meadows [30] or forests [31,32]. Narrowband indices acquired from spectrometric measurements are applicable for assessing vegetation vigor, e.g., chlorophyll concentration or change in pigment concentration during the growing season [33]. Hyperspectral data are commonly used for carrying out vegetation assessments in many valuable ecosystems, e.g., Yellowstone National Park [34], spectral properties of high Arctic plants [35], or modeling of heterogeneous grasslands [36].

The aim of this study is to assess how suitable narrow band vegetation indices are in assessing the chlorophyll concentration of three widespread and abundant high Arctic plants. A selection of indices allows us to limit the number of local surface measurements in favor of remote sensing-based monitoring, which can cover large areas. This is an important issue in the context of the approaching launch of the next two satellite missions, EnMAP [37] and FLEX [38]. The German spaceborne EnMAP mission will provide hyperspectral images in 230 bands (420–2,450 nm) with a ground resolution of 30 × 30 m. The swath width covers 30 × 5,000 km with a revisit of 4 days. One of the main goals of the EnMAP is to acquire biophysical and geochemical properties of the biogeosphere worldwide. ESA's FLEX mission in 2022 is for vegetation fluorescence mapping and analyzing. The system will orbit with a Copernicus Sentinel-3 satellite, which offers a swath width of 1,270–1,420 km, to integrate the optical and thermal properties of plants.

Research area and targets

The study area covers selected sites in the surroundings of Longyearbyen, which is the major settlement in the archipelago of Svalbard (78.2° N and 15.6° E). Longyearbyen is a former mining town. Hence, the landscape is contaminated with dust containing heavy metals [39–41]. The area is characterized by nutrient-rich soils and a maritime-buffered high Arctic climate with an average temperature for July and February of +5.9°C and −16.2°C, respectively [42]. The vegetation is dominated by moss-rich ferns and marshes in the lower parts of Adventdalen and by wind-exposed, dry dwarf shrub tundra in elevated areas (Fig. 1). The dominant species of the tundra are mountain avens (*Dryas octopetala* L.; Fig. 2), white arctic bell-heather [*Cassiope tetragona* (L.) D. Don], and polar willows (*Salix polaris* Wahlenb.; Fig. 3). Alpine bistort [*Bistorta vivipara* (L.) Delarbre] is one of the most abundant herbs in this tundra system. These species are pan-Arctic in distribution and widespread at Svalbard [42,43].

Dryas octopetala is a prostrate woody species (Fig. 2) forming a distinct heath community that grows in dry localities characterized by gravel and rocky barrens and where snow melts early [43,44]. It is semievergreen, meaning that chlorophyll in active leaves breaks down, the leaves become brown but overwinter attached to the shoots, and chlorophyll is reproduced in the same leaves the next spring [45]. *Salix polaris* is a prostrate mat-forming willow growing among gravel or in moss carpets (Fig. 2, Fig. 3). Fall leaf senescence generally starts early [43,44]. *Bistorta vivipara* is a perennial herb,

Fig. 1 View of one of the sites in Bjørndalen near Longyearbyen, Svalbard (photo: Z. Bochenek).

Fig. 2 Typical vegetation with polar willows (*Salix polaris*) in red and yellow and mountain avens (*Dryas octopetala*) in green (upper image; photo: Z. Bochenek). The lower image is *D. octopetala* (oblong, toothed green and yellow leaves) intermixed with *S. polaris* (rounded green leaves; photo: J. W. Bjerke).

Fig. 3 Polar willow (*Salix polaris*) on a carpet of mosses (photo: Z. Bochenek).

which in Svalbard, can be up to 15 cm tall under optimal conditions; however, it can grow on almost any substrate in Svalbard [43,44] and is often sterile (i.e., only producing basal leaves but no stalk).

Methods

The field campaign was carried out from August 4th to 7th in 2015 [35]. The following devices were used during the field research: (***i***) ASD FieldSpec 3 spectrometer connected with a fiber optic contact probe (ASD PlantProbe, which records the reflected electromagnetic radiation in the 350–2,500 nm range from the built-in lamp, providing stable conditions for all tested plants [46]) and (***ii***) Force-A Dualex Scientific sensor, which allows us to perform real-time and nondestructive measurements of chlorophyll (Chl), anthocyanins (Anth), flavonoids (Flav), and nitrogen (NBI) indices [47]. The chlorophyll index is highly correlated with the chlorophyll extracts measured in laboratory conditions (R^2 oscillated around 0.88–0.96 in hundreds of samples, and errors were not higher than 16%). Therefore, the presented chlorophyll index values are expressed as μg cm^{-2} [47].

The ASD FieldSpec 3 and Force-A Dualex Scientific have different sizes of sensors for measuring leaves; ASD PlantProbe measures a signal from an area of 2 cm in diameters and Force-A Dualex Scientific from an area of 5 mm in diameter. The recorded index values were not taken in the same leaves or plants, and the health status of the leaves was not documented in the field. So, data was collected from 10 different plants from the same sites with both instruments. For the spectrometric measurements, the size of the ASD PlantProbe detector required us to place smaller leaves next to each other, thus, chlorophyll concentrations were not tested in different parts of the leaves. This issue is not important in the case of upscaling field data to airborne or satellite levels. Each device was run 10 times at each site, with 10 spectrometric measurements consisting of 25 independent scans that were later averaged to one measurement, which in total gives 250 independent measurements for each species per site (Tab. 1).

Tab. 1 Location of the research sites and patterns (UTM, 33rd zone). In all sites, the following species were measured: *Salix polaris*, *Dryas octopetala*, and *Bistorta vivipara*.

Code	Name of the research site	*X* (m)	*Y* (m)
BOL_1	Bolterdalen	521,796	8,677,977
BOL_2		521,798	8,677,973
BOL_3		521,803	8,677,973
BOL_4		521,799	8,677,966
SVH_1	Svalbardhytta	519,620	8,679,379
SVH_2		519,629	8,679,373
SVH_3		519,628	8,679,368
SVH_4		519,621	8,679,369
ISD_1	Vest om Isdammen	516,085	8,682,454
ISD_2		516,083	8,682,446
ISD_3		516,082	8,682,435
ISD_4		516,066	8,682,442
YBJ_1	Ytre Bjørndalen	507,508	8,684,552
YBJ_2		507,510	8,684,545
YBJ_3		507,510	8,684,539
YBJ_4		507,507	8,684,530

The field-acquired spectrometric data was transferred to the ASD ViewSpec Pro software and exported as an ASCI file into the Statistica 13 software (StatSoft, Poland) to calculate the remote sensing indices (Tab. 2) by assessing the concentration of photosynthetic pigments in the vegetation and the amount of light used in the photosynthesis process (Tab. 3). At the same time, data from the chlorophyll measurements were imported into the Statistica software. We then used the Shapiro–Wilk test [48] to analyze the normality of the distributions of the calculated data. After that, the Levene test [49] to analyze the homogeneity of the variance was employed. Subsequently, the Kruskal–Wallis one-way analysis of variance by ranks (verification of the hypothesis about the irrelevance of differences between the medians of the tested variable in the populations, no normal distribution of the analyzed data [50]) was carried out for each species to check the statistical differences of the indices in individual sites at the significance level of $p < 0.05$. Then, a Tukey's test was used, which means that the sites were analyzed to verify which of them are different from the others in a statistically significant manner. Due to the nonparametric character of the data (no normal distribution), the Spearman's rank correlation coefficient [51] was determined for the vegetation indices, which was calculated from the spectral reflection curves that were correlated with the data from the measurements of the biophysical variables (pigment concentration), and the statistical significant was determined at the level of $p < 0.05$. This allowed for the determination of the remote sensing vegetation indices, which reflects the variability of the chlorophyll concentration of the analyzed species in a statistically significant manner.

Results

Quantitative measurements of chlorophyll concentration

The chlorophyll concentrations of the three species varied from site to site along the gradient from Ytre Bjørndalen to Bolterdalen. The highest average chlorophyll concentration was found in *S. polaris* with an average Chl index of 34.1, expressed as μg cm^{-2} [47]. The lowest average chlorophyll concentration was found in *D. octopetala* (average Chl index = 24.6). The lowest chlorophyll concentration for *D. octopetala* (Fig. 4) was found

Tab. 2 Overview of the vegetation indices that were applied to the collected data.

Index	Name	Formula	Reference
NDVI 705	Red edge normalized difference vegetation index	(*R*750 – *R*705) / (*R*750 + *R*705)	[59]
VOG 1	Vogelmann red edge index 1	*R*740 / *R*720	[60]
VOG 2	Vogelmann red edge index 2	(*R*734 – *R*747) / (*R*715 + *R*726)	[60]
VOG 3	Vogelmann red edge index 3	(*R*734 – *R*747) / (*R*715 + *R*720)	[60]
GM 2	Gitelson and Merzlyak index 2	*R*750 / *R*700	[22]
mND	Modified normalized difference index	((*R*750 to *R*900) – (*R*660 to *R*720)) / ((*R*750 to *R*900) + (*R*660 to *R*720) – 2*R*445)	[54]
RARSc	Ratio analysis of reflectance spectra algorithm carotenoid	*R*760 / *R*500	[61]
mNDVI 705	Modified normalized difference vegetation index 705	(*R*750 – *R*705) / (*R*750 + *R*705 – 2*R*445)	[54]
SIPI	Structure insensitive pigment index	(*R*800 – *R*445) / (*R*800 – *R*680)	[62]
PSRI	Plant senescence reflectance index	(*R*680 – *R*500) / *R*750	[63]
GNDVI	Green normalized difference vegetation index	(*NIR* – *GREEN*) / (*NIR* + *GREEN*)	[64]
GM1	Gitelson and Merzlyak indices 1	*R*750 / *R*550	[22]
NDVIred	Normalized difference vegetation index RED	(*R*780 – *R*680) / (*R*780 + *R*680)	[65]
NDVIgreen	Normalized difference vegetation index GREEN	(*R*780 – *R*570) / (*R*780 + *R*570)	[65]
ZMI	Zarco-Tejada and Miller	*R*750 / *R*710	[66]
LIC 1	Lichtenthaler indices 1	(*R*800 – *R*680) / (*R*800 + *R*680)	[67]
LIC 2	Lichtenthaler indices 2	*R*440 / *R*690	[67]
MTVI2	Modified triangular vegetation index	1.2 × (1.2 × (*R*800 – *R*550) – 2.5 × (*R*670 – *R*550))	[68]
MCARI2	Modified chlorophyll absorption ratio index improved	1.5 × (1.2 × (*R*800 – *R*670) – 1.3 × (*R*800 – *R*550)) / sqrt((2 × *R*800 + 1)^2 – (6 × *R*800 – 5 × sqrt(*R*670)) – 0.5)	[68]
GARI	Green atmospherically resistant index	(*NIR* – (*Green* – 0.5772156649 × (*Blue* – *Red*))) / (*NIR* + (*Green* – 0.5772156649 × (*Blue* – *Red*)))	[64]
GRVI	Green ratio vegetation index	*NIR* / *Green*	[69]
RGR	Red/green ratio; anthocyanins/chlorophyll	(*R*600 – *R*699) / (*R*500 – *R*599)	[70]
RARSa	Ratio analysis of reflectance spectra algorithm chlorophyll *a*	*R*675 / *R*700	[61]

in the SVH site (13.0), while the highest was found in the BOL site (47.0). The lowest chlorophyll concentration for *B. vivipara* was obtained in the SVH site (11.6), while the highest was found in the SVH (47.7) and BOL (48.0) sites. For the species *S. polaris*, the lowest chlorophyll concentration was in the SVH site (14.0), while the highest was found in the YBJ site (51.0). The highest variability amongst the chlorophyll concentrations was found in the SVH site (Fig. 4). There were not any significant intraspecific differences concerning chlorophyll content along the gradient taking into account the locations of the sites; the lowest average value for the Chl index was obtained in the SVH site (26.6), while the highest was found in the ISD site (31.4).

Vegetation indices

The vegetation indices extracted and calculated from the hyperspectral measurements were verified using Chl indices from the Dualex instrument. The calculated correlation (Spearman's rank correlation, *R* values) for the analyzed species was different at each research site. However, in the case of the analyzed species, high correlations between

Tab. 3 Application of the selected wavelengths for the plant pigment absorption analyzes via the hyperspectral analysis [71].

Wavelength (nm)	Application	Reference
439	Neoxanthin absorption analysis	[72]
443	Violaxanthin absorption analysis	[72]
445	Lutein absorption analysis	[72]
446	α-Carotene absorption analysis	[72]
463	β-Carotene absorption analysis	[72]
470	Carotenoids absorption analysis	[72]
530–630	Chlorophyll concentration analysis	[22]
531	Analysis of xanthophylls' cycles and energy absorption by thylakoids. The most used indicators: PRI (photochemical reflectance index) and LUE (photosynthetic light use efficiency).	[73]
540	Chlorophyll concentration analysis	[22]
550	Chlorophyll concentration analysis, chlorosis analysis range	[22]
555	Normalization of atmospheric effect's influence and AVI (angular vegetation index) analysis	[74]
570	Analysis of xanthophylls' cycles (similar to 531 nm range). Sensitive for chlorophyll concentration.	[73]
650	Chlorosis analysis	[75]
663.2	Chlorophyll *a* absorption	[76]
646.8	Chlorophyll *b* absorption	[76]
670	Normalization of soil effect's influence and AVI analysis. Band for low chlorophyll concentration analysis.	[74]
680	Chlorophyll absorption	[77]
695	PSI (plant stress index) 760/695 nm	[78]
697–713	Deciduous' trees branches analysis	[79]
680	Chlorophyll concentration analysis	[23]
690	Chlorophyll concentration analysis	[22]
696–733	Deciduous' trees analysis	[80]
700	Chlorophyll concentration analysis	[22]
703, 704	Red edge inflection (plant stress analysis)	[81]
710	Chlorophyll concentration analysis	[22]
719	Red edge inflection (plant stress analysis)	[81]
750, 754	Red edge inflection (plant stress analysis)	[23]
760/695	Plant stress index	[78]
842–950	Deciduous' trees analysis	[82]
850	Chlorophyll concentration analysis	[23]

parameters of the indices were confirmed (statistically significant values at the significance level of $p < 0.05$ are marked in bold in Tab. 4).

As the sites were located in different places and thus characterized by different environmental conditions, statistically significant differences (at the significance level of $p < 0.05$) were observed among the index values. Out of all the research sites containing the analyzed species, the most numerously represented indices that showed statistically significant changes were: VOG 1, ZMI, mNDVI, mND, VOG 2, VOG 3, and NDVI 705. This allowed us to narrow down the analyzes to those indices that best represent the condition of the vegetation (highest percentage) and to confirm it with the values and strong correlations of the chlorophyll measurements (Tab. 4).

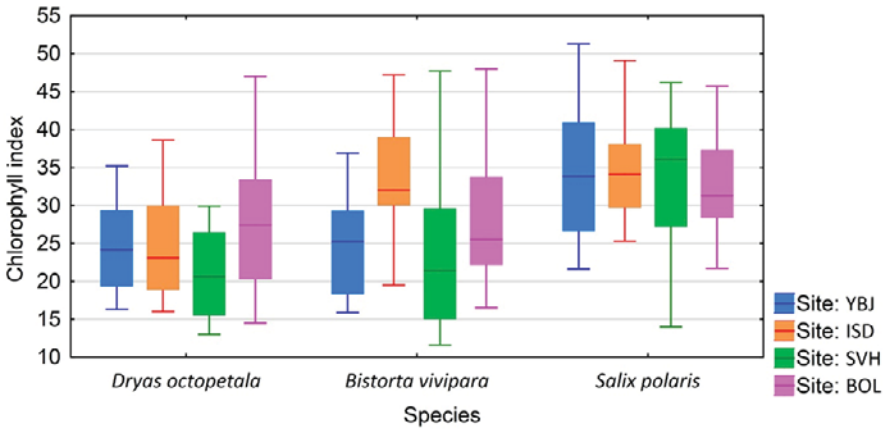

Fig. 4 Chlorophyll concentrations (maximum, minimum, median, and upper and lower percentiles) of *D. octopetala*, *B. vivipara*, and *S. polaris* along a gradient with decreasing oceanicity at Spitsbergen for the sites YBJ, ISD, BOL, and SVH. Values of the chlorophyll index are expressed as μg cm^{-2} [47].

Tab. 4 Relationship between optically measured chlorophyll concentration and various vegetation index values.

Index	*Salix polaris*	*Dryas octopetala*	*Bistorta vivipara*
VOG 1	**0.66**	0.20	**0.53**
ZMI	**0.52**	0.20	**0.61**
mNDVI 705	**0.56**	0.14	**0.57**
mND	**0.59**	0.12	**0.51**
VOG 2	**−0.54**	−0.24	**−0.55**
VOG 3	**−0.54**	−0.23	**−0.55**
NDVI 705	**0.50**	0.19	**0.58**
GM 2	**0.47**	0.18	**0.59**
LIC 2	**0.58**	−0.17	**0.48**
SIPI	−0.31	0.12	**−0.46**
GARI	0.19	0.16	**0.46**
PSRI	**−0.54**	0.03	−0.09
MTVI2	0.30	0.02	0.19
MCARI2	0.30	0.02	0.19
LIC 1	0.25	−0.04	0.09
PSSRa	0.25	−0.04	0.08
RARSc	0.19	0.24	0.07
GRVI	0.02	0.21	0.02
GM 1	0.03	0.19	−0.08
GNDVI	−0.01	0.17	−0.07
NDVIred	0.25	−0.04	−0.44
RGR	−0.26	0.28	0.00
NDVIgreen	0.04	0.23	−0.31

Numbers in bold are statistically significant (Spearman's rank $p < 0.05$).

A significant number of remote sensing indices indicated a chlorophyll concentration based on these same ranges (covering blue, green, and red ranges), so most of them are highly correlated (Fig. 5). For future analyzes, these indices that have the highest values of correlation, e.g., NDVI 705 and VOG 1, 2, 3, GM 2, mND, or mNDVI 705 (first column in Fig. 5) should not be selected because this same set of information would be duplicated.

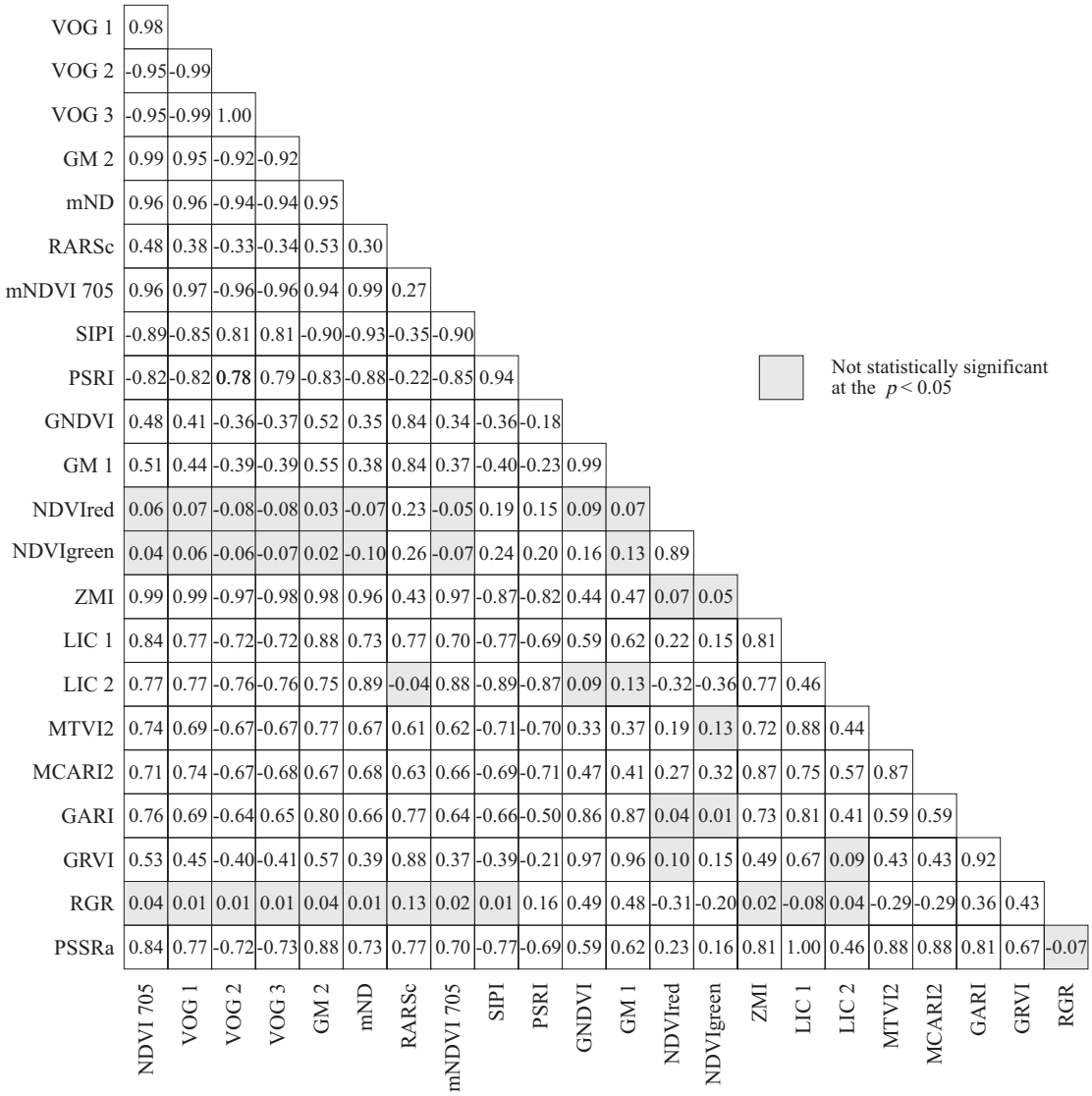

Fig. 5 A correlation matrix between different remote sensing indices derived from ASD FieldSpec measurements (N = 160 averages of 4,000 independent measurements). Full names of the indices are presented in the Tab. 2.

Better indices for selection are NDVI 705 and GNDVI, GM 1, or GRVI (which are statistically significant, but the chlorophyll concentration information does not overlap). A proper analysis should be based on a sensor filter range of full width at half maximum (FWHM; technical data including the values of used wavelengths are presented on sensor web pages) because not all sensors have the same ranges as the used bands, thus, not all presented indices in Fig. 5 could be calculated from all sensors. This problem is solved during airborne hyperspectral missions via the satellite's Hyperion or oncoming EnMAP scanners.

One of the most commonly used indices from the narrowband group is the NDVI 705 index. The present research confirms that *S. polaris* and *B. vivipara* had the highest values and the highest amount of chlorophyll of the species in the analyzed sites (0.49 and 0.48, respectively), while *D. octopetala* had the lowest results (0.35) in the same

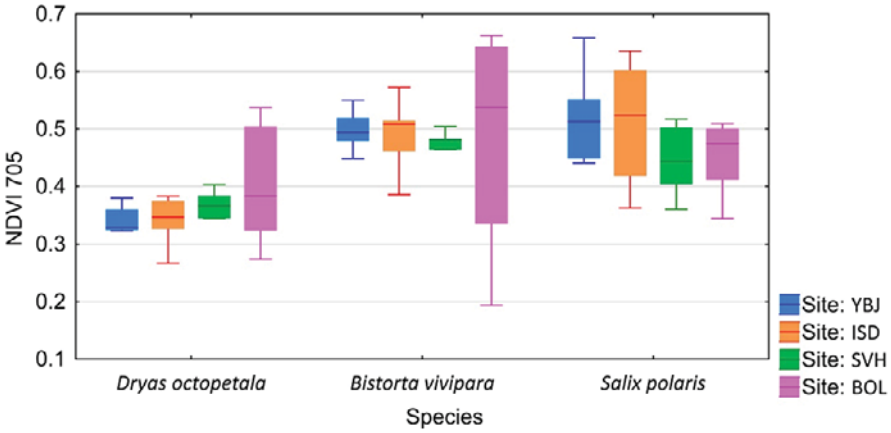

Fig. 6 The values of the NDVI 705 index (maximum, minimum, median, and upper and lower percentiles) for the species *D. octopetala*, *B. vivipara*, and *S. polaris* in the YBJ, ISD, SVH, and BOL sites.

sites (Fig. 6). There is a significant difference between *D. octopetala* and *B. vivipara* for the sites YBJ, ISD, and SVH, while there was a significant difference between *D. octopetala* and *S. polaris* for the site YBJ. However, there were no intraspecific significant differences between sites.

The mNDVI 705 index, which is a modification of the NDVI (a broadband index) or NDVI 705 (a narrowband index), also allowed us to indicate the level of chlorophyll concentration in *S. polaris* and *B. vivipara*. Both species had the highest values (averages = 0.56) and the highest amount of chlorophyll of the species in the analyzed sites, while *D. octopetala* had the lowest results (0.42) in the same sites (Fig. 7). There is a significant difference between *D. octopetala* and *B. vivipara* for the YBJ, ISD, and SVH sites, while there was a significant difference between *D. octopetala* and *S. polaris* for the YBJ site. However, there were no intraspecific significant differences between sites.

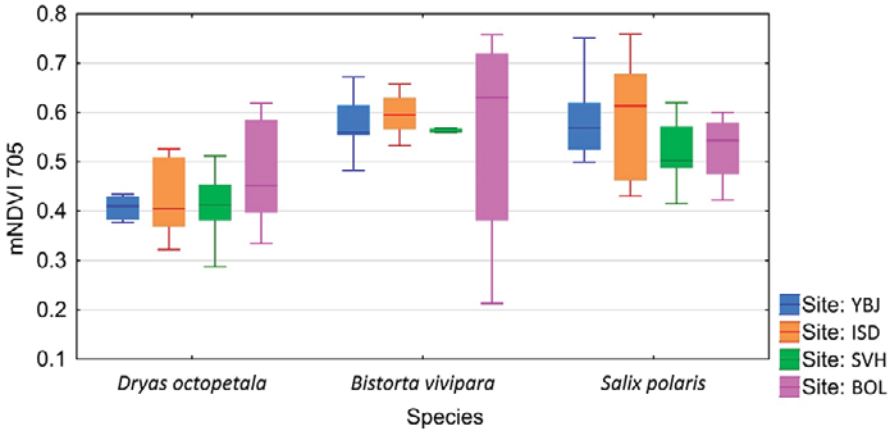

Fig. 7 The values of the mNDVI 705 index (maximum, minimum, median, and upper and lower percentiles) for the species *D. octopetala*, *B. vivipara* and *S. polaris* in the YBJ, ISD, SVH, and BOL sites.

The VOG 1, 2, 3 indices (there should be a negative relationship between the VOG 1, VOG 2, and VOG 3 indices; Fig. 5) indicate a similar relationship for the three species studied in the different sites. Hence, each of the analyzed indices confirms in a statistically significant way the chlorophyll concentration levels. The VOG 1 index (Fig. 8–Fig. 10) also had the highest values for *S. polaris* and the lowest for *D. octopetala*, similar to what was observed for NDVI 705.

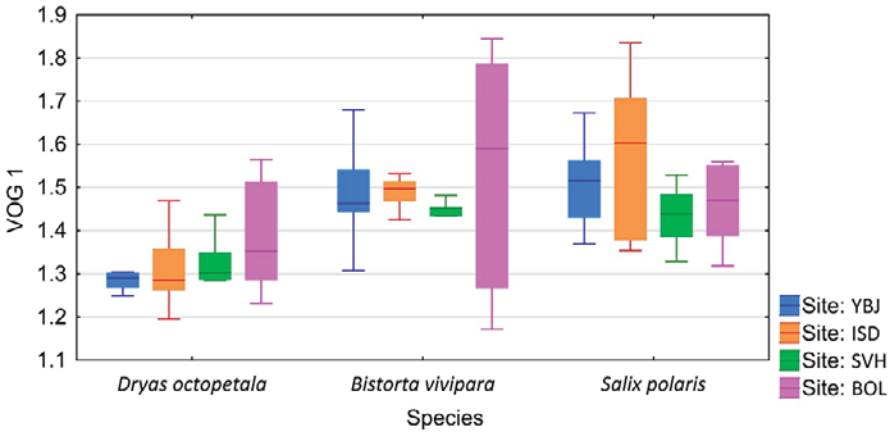

Fig. 8 The values of the VOG 1 index (maximum, minimum, median, and upper and lower percentiles) for the species *D. octopetala*, *B. vivipara*, and *S. polaris* in the YBJ, ISD, SVH, and BOL sites.

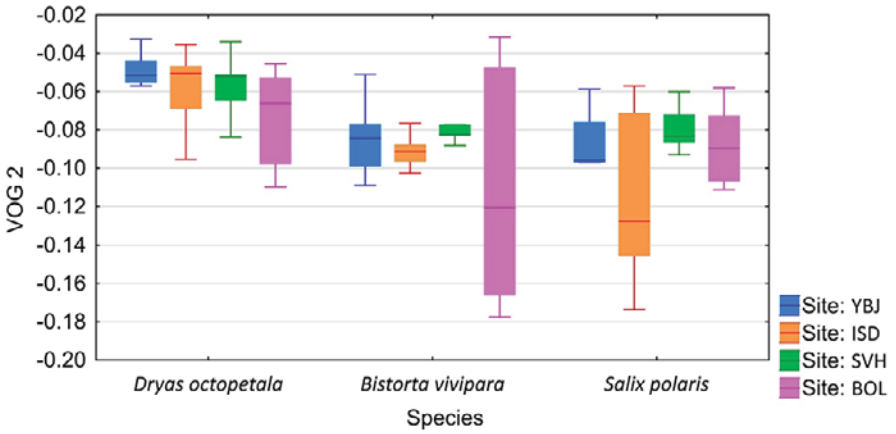

Fig. 9 The values of the VOG 2 index (maximum, minimum, median, and upper and lower percentiles) for the species *D. octopetala*, *B. vivipara*, and *S. polaris* in the YBJ, ISD, SVH, and BOL sites.

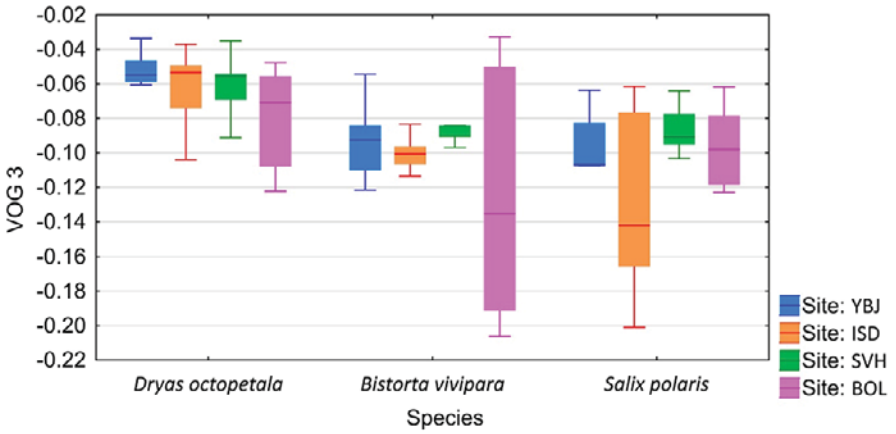

Fig. 10 The values of the VOG 3 index (maximum, minimum, median, and upper and lower percentiles) for the species *D. octopetala*, *B. vivipara*, and *S. polaris* in the YBJ, ISD, SVH, and BOL sites.

The other two indices, VOG 2 and VOG 3, confirm the data reported above. Because they are indices that are interpreted inversely, *Salix polaris* had the lowest values on the graph, while *Dryas octopetala* had the highest value (Fig. 9, Fig. 10).

As the mND index was developed for the wavelengths of 750–900 nm, 660–720 nm, and 445 nm, it is very good at illustrating the radiation absorption by pigments and, therefore, also determining the chlorophyll concentration levels. This confirms the above-described observations, i.e., the highest values of the index were for *S. polaris*, the medium-level values were for *B. vivipara*, and the lowest values were for *D. octopetala* in the YBJ, ISD, and SVH sites. In the BOL site, the highest values were for *B. vivipara* (Fig. 11).

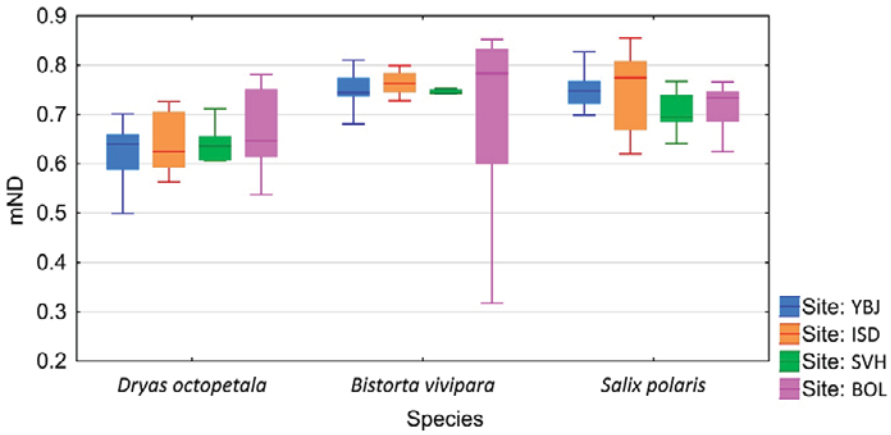

Fig. 11 The values of the mND index (maximum, minimum, median, and upper and lower percentiles) for the species *D. octopetala*, *B. vivipara*, and *S. polaris* in the YBJ, ISD, SVH, and BOL sites.

As the ZMI index was developed for the wavelengths of 750 and 710 nm, it is very good at illustrating the radiation absorption by pigments and, therefore, also determining the chlorophyll concentration levels and cellular structures. This confirms the above-described observations, i.e., the highest values of the index were for *S. polaris*, the medium-level values were for *B. vivipara*, and the lowest values were for *D. octopetala* in the YBJ, ISD, and SVH sites. In the BOL site, the highest values were for *B. vivipara* (Fig. 12).

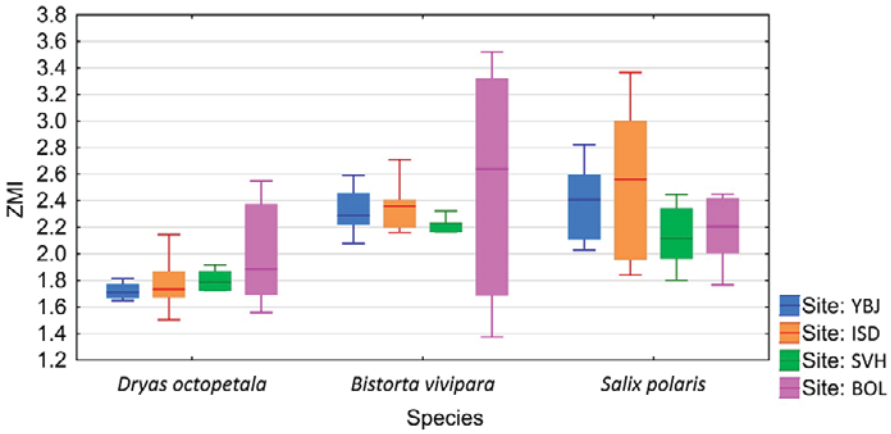

Fig. 12 The values of the ZMI index (maximum, minimum, median, and upper and lower percentiles) for the species *D. octopetala*, *B. vivipara*, and *S. polaris* in the YBJ, ISD, SVH, and BOL sites.

Discussion

The selection of vegetation indices in this study confirmed that the most applicable indices for all species were VOG 1, ZMI, mNDVI, mND, VOG 2, VOG 3, and NDVI 705. There were also less, but strong, relationships between the chlorophyll measurements and the vegetation indices of chlorophyll levels above 0.5 for the following indices: GM 2, LIC 2, SIPI, GARI, and PSRI. It should also be mentioned that for the plants in the alpine zone of the Tatras, the NDVI 705 and VOG 1, 2, 3 indices were statistically significant in 87.5% of cases [52], while the GM 2 index was statistically significant in 69% of cases, and RARSc in 71% [52]. Other important vegetation indices of the alpine zone included: RARS (80%), GI (77%), and LIC 2, mNDVI 705, RGR, and SRPI in 70% of analyzed species [53].

For the best mND, the average correlation coefficient for all species was 0.41 (Tab. 4), while *S. polaris* showed the best result in all individual species: 0.59. For *B. vivipara*, the value was 0.51. Slightly better results were obtained in laboratory conditions by Sims and Gamon [54] as the mND index correlated with the chlorophyll concentration (0.6 mmol m^{-2}) at the R^2 level of 0.62–0.66 (nonlinear models). On the other hand, the results for the NDVI 705 index (not including the 445 nm wavelength) ranged from 0.50 to 0.58 (excluding 0.19 of *D. octopetala*) with the above-mentioned chlorophyll concentration level [54]. In all of the above cases (concerning both this study and the cited publications), the relationships were statistically significant. The above-referenced studies [54] were used for the assessment of vegetation greenness and ecosystem CO_2 exchange in response to a drought in the Southern California chaparral ecosystem [55]. Analyzes based on surface and airborne ADAR imager measurements (captures the relationship between CO_2 accumulation and chlorophyll activity) in the field (chlorophyll content index – CCI) were calculated from the image NDVI 705 at $R^2 = 0.85$ [55].

Hope et al. [56] achieved similar results measuring Alaskan tundra plants (three vegetation communities); hand-held radiometer data of 5 × 5 m point-quadrat estimates of the photosynthetic active biomass sites correlated with NDVI vegetation indices, which were adapted to the parameters of satellite images of Landsat and SPOT. The nonlinear correlation force (R^2) of the indices ranged from 0.48 to 0.52 [56]. Significantly stronger relationships between NDVI indices (e.g., NDVI 705 and GNDVI) can be observed in the case of agricultural crops [57]; correlations between the vegetation indices and the surface chlorophyll measurements reached $R^2 = 0.95$ [55], e.g., for NDVI 705, chlorophyll = 0.86 (soybean) and 0.94 (maize). In this study, the values are lower by almost a half (0.41–0.63). In the case of the GNDVI index, the correlation values were 0.88 for soybean and 0.85 for maize (in this study, the correlation coefficients were 0.46–0.57). It should be remembered that polar plants are covered with waxes and other layers that protect them against winter warming events that may lead to drying and freezing. These elements significantly reduce the possibilities of chlorophyll identification [58]. Further assessment of the results from the analysis indicated that the species *S. polaris* and *B. vivipara* were in very good to good condition, while *D. octopetala* was in medium condition. There were also differences between the sites, and the variability within sites was high, especially in the site BOL, indicating that the environmental conditions differed. These results are in accordance with results by Zagajewski et al. [35] and Bjerke et al. [39], which showed that the health condition was lower for *D. octopetala* compared to that of *S. polaris* and *B. vivipara* due to different climatic and contaminant conditions (mining) within the study area [41].

Conclusions

The analyzes of the dominant Svalbard species showed that their chlorophyll concentration levels were within the optimal range for *S. polaris* and *B. vivipara*; attention was paid to the variability of these values, depending on the species and sites.

Simultaneous spectral and chlorophyll concentration-focused analyzes confirmed the statistical significance of individual narrow-band vegetation indices. The most optimal indices were: VOG 1, ZMI, mNDVI, mND, VOG 2, VOG 3, and NDVI 705. This is an important factor in the context of new satellite missions, e.g., Sentinel,

EnMAP, or FLEX. Although the observed relationships were not very strong, the use of hyperspectral data for the monitoring of vast areas of the Arctic will allow for the observation of trends regarding changes in vegetation and the continuous monitoring of the Arctic greening process. Use of satellite remote sensing supported by periodic biometric surface measurements conducted in permanent sites will be valuable for vegetation monitoring in the high Arctic.

References

1. Swain PH, Davis SM. Remote sensing: the quantitative approach. New York, NY: McGraw-Hill Inc.; 1987.
2. Roy PS. Spectral reflectance characteristics of vegetation and their use in estimating productive potential. Proceedings: Plant Sciences. 1989;99(1):59–81.
3. Asner GP. Biophysical and biochemical sources of variability in canopy reflectance. Remote Sens Environ. 1998;64(3):234–253. https://doi.org/10.1016/S0034-4257(98)00014-5
4. Schaepman-Strub G, Schaepman ME, Painter TH, Dangel S, Martonchik JV. Reflectance quantities in optical remote sensing – definitions and case studies. Remote Sens Environ. 2006;103(1):27–42. https://doi.org/10.1016/j.rse.2006.03.002
5. Gates DM, Keegan HJ, Schleter JC, Weidner VR. Spectral properties of plants. Appl Opt. 1965;4(1):11–20. https://doi.org/10.1364/AO.4.000011
6. Jensen JR. Biophysical remote sensing – review article. Ann Assoc Am Geogr. 1983;73(1):111–132. https://doi.org/10.1111/j.1467-8306.1983.tb01399.x
7. Clevers JGPW, Kooistra L, Schaepman ME. Estimating canopy water content using hyperspectral remote sensing data. Int J Appl Earth Obs Geoinf. 2010;12(2):119–125. https://doi.org/10.1016/j.jag.2010.01.007
8. Zhang M, Ustin SL, Rejmankova E, Sanderson EW. Monitoring pacific coast salt marshes using remote sensing. Ecol Appl. 1997;7(3):1019–1053. https://doi.org/10.1890/1051-0761(1997)007[1039:MPCSMU]2.0.CO;2
9. Thomas JR, Oerther GF. Estimating nitrogen content of sweet pepper leaves by reflectance measurements. Agron J. 1972;64:11–13. https://doi.org/10.2134/agronj1972.00021962006400010004x
10. Gausman HW, Allen WA, Cardenas R. Reflectance of cotton leaves and their structure. Remote Sens Environ. 1969;1:19–22. https://doi.org/10.1016/S0034-4257(69)90055-8
11. Gausman HW, Allen WA, Wiegand CL, Escobar DE, Rodrigues RR, Richardson AJ. The leaf mesophyll of twenty crops, their light spectra and optical and geometrical parameters. Weslaco, TX: USDA, Agricultural Research Service, Soil and Water Conservation Research Division, Rio Grande Soil and Water Research Center; 1971. (SWC Research Report; vol 423). https://doi.org/10.5962/bhl.title.149765
12. Kycko M, Zagajewski B, Lavender S, Romanowska E, Zwijacz-Kozica M. The impact of tourist traffic on the condition and cell structures of alpine swards. Remote Sens. 2018;10(2):220. https://doi.org/10.3390/rs10020220
13. Richardson AD, Duigan SP, Berlyn GP. An evaluation of noninvasive methods to estimate foliar chlorophyll content. New Phytol. 2002;153(1):185–194. https://doi.org/10.1046/j.0028-646X.2001.00289.x
14. Gitelson AA. Wide dynamic range vegetation index for remote quantification of biophysical characteristics of vegetation. J Plant Physiol. 2004;161(2):165–173. https://doi.org/10.1078/0176-1617-01176
15. Arena C, Vitale L, de Santo AV. Paraheliotropism in *Robinia pseudoacacia* L.: an efficient strategy to optimise photosynthetic performance under natural environmental conditions. Plant Biol. 2008;10(2):194–201. https://doi.org/10.1111/j.1438-8677.2008.00032.x
16. Olascoaga B, Juurola E, Lukeš P, Nikinmaa E, Bäck J, Porcar-Castell A, et al. Seasonal variation in the reflectance of photosynthetically active radiation from epicuticular waxes of Scots pine (*Pinus sylvestris*) needles. Boreal Environ Res. 2014;19(suppl B):132–141. https://doi.org/10.1007/s10534-014-9780-1

17. Merzlyak MN, Chivkunova OB, Solovchenko AE, Naqvi KR. Light absorption by anthocyanins in juvenile, stressed, and senescing leaves. J Exp Bot. 2008;59(14):3903–3911. https://doi.org/10.1093/jxb/ern230

18. Porcar-Castell A, Tyystjärvi E, Atherton J, van der Tol C, Flexas J, Pfündel EE, et al. Linking chlorophyll *a* fluorescence to photosynthesis for remote sensing applications: mechanisms and challenges. J Exp Bot. 2014;65(15):4065–4095. https://doi.org/10.1093/jxb/eru191

19. Kalaji HM, Bosa K, Kościelniak J, Hossain Z. Chlorophyll *a* fluorescence – a useful tool for the early detection of temperature stress in spring barley (*Hordeum vulgare* L.). OMICS: A Journal of Integrative Biology. 2011;15(12):925–934. https://doi.org/10.1089/omi.2011.0070

20. Porcar-Castell A, Garcia-Plazaola JI, Nichol CJ, Kolari P, Olascoaga B, Kuusinen N, et al. Physiology of the seasonal relationship between the photochemical reflectance index and photosynthetic light use efficiency. Oecologia 2012;170(2):313. https://doi.org/10.1007/s00442-012-2317-9

21. Zarco-Tejada PJ, González-Dugo V, Berni JAJ. Fluorescence, temperature and narrow-band indices acquired from a UAV platform for water stress detection using a micro-hyperspectral imager and a thermal camera. Remote Sens Environ. 2012;117:322–337. https://doi.org/10.1016/j.rse.2011.10.007

22. Gitelson AA, Merzlyak MN. Remote estimation of chlorophyll content in higher plant leaves. Int J Remote Sens. 1997;18(12):2691–2697. https://doi.org/10.1080/014311697217558

23. Datt B. A new reflectance index for remote sensing of chlorophyll content in higher plants: tests using eucalyptus leaves. J Plant Physiol. 1999;154(1):30–36. https://doi.org/10.1016/S0176-1617(99)80314-9

24. Zhu XG, Govindjee, Baker NR, DeSturler E, Ort DR, Long SP. Chlorophyll *a* fluorescence induction kinetics in leaves predicted from a model describing each discrete step of excitation energy and electron transfer associated with photosystem II. Planta. 2005;223(1):114–133. https://doi.org/10.1007/s00425-005-0064-4

25. Tan CW, Wang DL, Zhou J, Du Y, Luo M, Zhang YL, et al. Assessment of F_v/F_m absorbed by wheat canopies employing in-situ hyperspectral vegetation indexes. Sci Rep. 2018;8:9525. https://doi.org/10.1038/s41598-018-27902-3

26. Cierniewski J, Kazmierowski C, Krolewicz S, Piekarczyk J, Wrobel M, Zagajewski B. Effects of different illumination and observation techniques of cultivated soils on their hyperspectral bidirectional measurements under field and laboratory conditions. IEEE J Sel Top Appl Earth Obs Remote Sens. 2014;7(6):2525–2530. https://doi.org/10.1109/JSTARS.2014.2298098

27. Cierniewski J, Ceglarek J, Karnieli A, Królewicz S, Kaźmierowski C, Zagajewski B. Predicting the diurnal blue-sky albedo of soils using their laboratory reflectance spectra and roughness indices. J Quant Spectrosc Radiat Transf. 2017;200:25–31. https://doi.org/10.1016/j.jqsrt.2017.05.033

28. Rossini M, Fava F, Cogliati S, Meroni M, Marchesi A, Panigada C, et al. Assessing canopy PRI from airborne imagery to map water stress in maize. ISPRS J Photogramm Remote Sens. 2013;86:168–177. https://doi.org/10.1016/j.isprsjprs.2013.10.002

29. Wieneke S, Ahrends H, Damm A, Pinto F, Stadler A, Rossini M, et al. Airborne based spectroscopy of red and far-red sun-induced chlorophyll fluorescence: implications for improved estimates of gross primary productivity. Remote Sens Environ. 2016;184:654–667. https://doi.org/10.1016/j.rse.2016.07.025

30. Marcinkowska-Ochtyra A, Zagajewski B, Raczko E, Ochtyra A, Jarocińska A. Classification of high-mountain vegetation communities within a diverse giant mountains ecosystem using airborne APEX hyperspectral imagery. Remote Sens. 2018;10(4):570. https://doi.org/10.3390/rs10040570

31. Raczko E, Zagajewski B. Tree species classification of the UNESCO Man and the Biosphere Karkonoski National Park (Poland) using artificial neural networks and APEX hyperspectral images. Remote Sens. 2018;10(7):1111. https://doi.org/10.3390/rs10071111

32. Hawryło P, Bednarz B, Wężyk P, Szostak M. Estimating defoliation of Scots pine stands using machine learning methods and vegetation indices of Sentinel-2. Eur J Remote Sens. 2018;51(1):194–204. https://doi.org/10.1080/22797254.2017.1417745

33. Marshall M, Thenkabail P, Bigges T, Post K. Hyperspectral narrowband and multispectral broadband indices for remote sensing of crop evapotranspiration and its components

(transpiration and soil evaporation). Agric For Meteorol. 2015;218–219:122–134. https://doi.org/10.1016/j.agrformet.2015.12.025

34. Aspinall R. Use of logistic regression for validation of maps of the spatial distribution of vegetation species derived from high spatial resolution hyperspectral remotely sensed data. Ecol Model. 2002;157:301–312. https://doi.org/10.1016/S0304-3800(02)00201-6
35. Zagajewski B, Tømmervik H, Bjerke JW, Raczko E, Bochenek Z, Kłos A, et al. Intraspecific differences in spectral reflectance curves as indicators of reduced vitality in high-arctic plants. Remote Sens. 2017;9(12):1289. http://doi.org/10.3390/rs9121289
36. Darvishzadeh R, Skidmore A, Schlerf M, Atzberger C, Corsi F, Cho M. LAI and chlorophyll estimation for a heterogeneous grassland using hyperspectral measurements. ISPRS J Photogramm Remote Sens. 2008;63(4):409–426. https://doi.org/10.1016/j.isprsjprs.2008.01.001
37. Guanter L, Kaufmann H, Segl K, Foerster S, Rogass C, Chabrillat S, et al. The EnMAP spaceborne imaging spectroscopy mission for Earth observation. Remote Sens. 2015;7:8830–8857. https://doi.org/10.3390/rs70708830
38. Moreno J, Alonso L, Delegido J, Rivera JP, Ruiz-Verdú A, Sabater N, et al. FLEX (Fluorescence Explorer) mission: observation fluorescence as a new remote sensing technique to study the global terrestrial vegetation state. Revista de Teledetección. 2014;41:111–119. https://doi.org/10.4995/raet.2014.2296
39. Bjerke JW, Treharne R, Vikhamar-Schuler D, Karlsen SR, Ravolainen V, Bokhorst S, et al. Understanding the drivers of extensive plant damage in boreal and Arctic ecosystems: insights from field surveys in the aftermath of damage. Sci Total Environ. 2017;599–600:1965–1976. https://doi.org/10.1016/j.scitotenv.2017.05.050
40. Kłos A, Bochenek Z, Bjerke JW, Zagajewski B, Ziółkowski D, Ziembik Z, et al. The use of mosses in biomonitoring of selected areas in Poland and Spitsbergen in the years from 1975 to 2014. Ecological Chemistry and Engineering S. 2015;22(2):201–218. https://doi.org/10.1515/eces-2015-0011
41. Kłos A, Ziembik Z, Rajfur M, Dolhanczuk-Środka A, Bochenek Z, Bjerke JW, et al. The origin of heavy metals and radionuclides accumulated in the soil and biota samples collected in Svalbard, near Longyearbyen. Ecological Chemistry and Engineering S. 2017;24;223–238. https://doi.org/10.1515/eces-2017-0015
42. Johansen B, Tømmervik H. The relationship between phytomass, NDVI and vegetation communities on Svalbard. Int J Appl Earth Obs Geoinf. 2014;27(A):20–30. https://doi.org/10.1016/j.jag.2013.07.001
43. Rønning O. The flora of Svalbard. Oslo: Norwegian Polar Institute; 1996. (Polarhåndbok; vol 10).
44. Johansen BE, Karlsen SR, Tømmervik H. Vegetation mapping of Svalbard utilising Landsat TM/ETM+ data. Polar Rec. 2012:48:47–63. https://doi.org/10.1017/S0032247411000647
45. Welker JM, Molau U, Parsons AN, Robinson CH, Wookey PA. Responses of *Dryas octopetala* to ITEX environmental manipulations: a synthesis with circumpolar comparisons. Glob Chang Biol. 1997;3(S1):61–73. https://doi.org/10.1111/j.1365-2486.1997.gcb143.x
46. Potůčková M, Červená L, Kupková L, Lhotáková Z, Lukeš P, Hanuš J, et al. Comparison of reflectance measurements acquired with a contact probe and an integration sphere: implications for the spectral properties of vegetation at a leaf level. Sensors. 2016;16:1801. https://doi.org/10.3390/s16111801
47. Cerovic ZG, Masdoumier G, Ben Ghozlen N, Latouche G. A new optical leaf-clip meter for simultaneous non-destructive assessment of leaf chlorophyll and epidermal flavonoids. Physiol Plant. 2012;146(3):251–260. https://doi.org/10.1111/j.1399-3054.2012.01639.x
48. Shapiro SS, Wilk MB. An analysis of variance test for normality (complete samples). Biometrika. 1965;52(3–4):591. https://doi.org/10.2307/2333709
49. Lehmann EL, Romano JP. Testing statistical hypotheses. 3rd ed. New York, NY: Springer; 2005.
50. Kruskal WH. A nonparametric test for the several sample problem. Annals of Mathematical Statistics. 1952;23:525–540. https://doi.org/10.1214/aoms/1177729332
51. Spearman Ch. The proof and measurement of association between two things. Am J Psychol. 1904;15:72–101. https://doi.org/10.2307/1412159

52. Kycko M, Zagajewski B, Zwijacz-Kozica M, Cierniewski J, Romanowska E, Orłowska K, et al. Assessment of hyperspectral remote sensing for analyzing the impact of human trampling on alpine swards. Mt Res Dev. 2017;37(1):66–74. https://doi.org/10.1659/MRD-JOURNAL-D-15-00050.1

53. Kycko M. Assessment of the dominant alpine sward species condition of the Tatra National Park using hyperspectral remote sensing [PhD thesis]. Warsaw: Faculty of Geography and Regional Studies, University of Warsaw; 2017.

54. Sims DA, Gamon JA. Relationships between leaf pigment content and spectral reflectance across a wide range of species, leaf structures and developmental stages. Remote Sens Environ. 2002;81(2–3):337–354. https://doi.org/10.1016/S0034-4257(02)00010-X

55. Sims D, Luo H, Hastings S, Oechel W, Rahman A, Gamon J. Parallel adjustments in vegetation greenness and ecosystem CO_2 exchange in response to drought in a Southern California chaparral ecosystem. Remote Sens Environ. 2006;103(3):289–303. https://doi.org/10.1016/j.rse.2005.01.020

56. Hope AS, Kimball JS, Stow DA. The relationship between tussock tundra spectral reflectance properties and biomass and vegetation composition, Int J Remote Sens. 1993;14(10):1861–1874. https://doi.org/10.1080/01431169308954008

57. Peng Y, Nguy-Robertson A, Arkebauer T, Gitelson AA. Assessment of canopy chlorophyll content retrieval in maize and soybean: implications of hysteresis on the development of generic algorithms. Remote Sens. 2017;9:226. https://doi.org/10.3390/rs9030226

58. Shepherd T, Wynne Griffiths D. The effects of stress on plant cuticular waxes. New Phytol. 2006;171(3):469–499. https://doi.org/10.1111/j.1469-8137.2006.01826.x

59. Gitelson A, Merzlyak MN. Quantitative estimation of chlorophyll-*a* using reflectance spectra: experiments with autumn chestnut and maple leaves. J Photochem Photobiol B. 1994;22(3):247–252. https://doi.org/10.1016/1011-1344(93)06963-4

60. Vogelmann JE, Rock BN, Moss DM. Red edge spectral measurements from sugar maple leaves. Int J Remote Sens. 1993;14(8):1563–1575. https://doi.org/10.1080/01431169308953986

61. Chappelle EW, Kim MS, McMurtrey JE. Ratio analysis of reflectance spectra (RARS): an algorithm for the remote estimation of the concentrations of chlorophyll *a*, chlorophyll *b*, and carotenoids in soybean leaves. Remote Sens Environ. 1992;39(3):239–247. https://doi.org/10.1016/0034-4257(92)90089-3

62. Peñuelas J, Baret F, Filella I, Penuelas J, Baret F, Filella I. Semiempirical indexes to assess carotenoids chlorophyll-*a* ratio from leaf spectral reflectance. Photosynthetica. 1995;31(2):221–230.

63. Merzlyak MN, Gitelson AA, Chivkunova OB, Rakitin VY. Non-destructive optical detection of pigment changes during leaf senescence and fruit ripening. Physiol Plant. 1999;106(1):135–141. https://doi.org/10.1034/j.1399-3054.1999.106119.x

64. Gitelson AA, Kaufman YJ, Merzlyak MN. Use of a green channel in remote sensing of global vegetation from EOS-MODIS. Remote Sens Environ. 1996;58(3):289–298. https://doi.org/10.1016/S0034-4257(96)00072-7

65. Mänd P, Hallik L, Peñuelas J, Nilson T, Duce P, Emmett BA, et al. Responses of the reflectance indices PRI and NDVI to experimental warming and drought in European shrublands along a north–south climatic gradient. Remote Sens Environ. 2010;114:626–636. https://doi.org/10.1016/j.rse.2009.11.003

66. Zarco-Tejada PJ, Miller JR, Mohammed GH, Noland TL, Sampson PH. Estimation of chlorophyll fluorescence under natural illumination from hyperspectral data. Int J Appl Earth Obs Geoinf. 2001;3(4):321–327. https://doi.org/10.1016/S0303-2434(01)85039-X

67. Lichtenthaler HK, Lang M, Sowinska M, Heisel F, Miehé JA. Detection of vegetation stress via a new high resolution fluorescence imaging system. J Plant Physiol. 1996;148(5):599–612. https://doi.org/10.1016/S0176-1617(96)80081-2

68. Haboudane D. Hyperspectral vegetation indices and novel algorithms for predicting green LAI of crop canopies: modeling and validation in the context of precision agriculture. Remote Sens Environ. 2004;90:337–352. https://doi.org/10.1016/j.rse.2003.12.013

69. Sripada RP, Heiniger RW, White JG, Meijer AD. Aerial color infrared photography for determining early in-season nitrogen requirements in corn. Agron J. 2006;98:968–977. https://doi.org/10.2134/agronj2005.0200

70. Fuentes DA, Gamon JA, Qiu H, Sims DA, Roberts DA. Mapping Canadian

boreal forest vegetation using pigment and water absorption features derived from the AVIRIS sensor. J Geophys Res Atmos. 2001;106(D24):33565–33577. https://doi.org/10.1029/2001JD900110

71. Zagajewski B. Ocena przydatności sieci neuronowych i danych hiperspektralnych do klasyfikacji roślinności Tatr Wysokich. Warszawa: Klub Teledetekcji Środowiska Polskiego Towarzystwa Geograficznego; 2010. (Teledetekcja Środowiska; vol 43).
72. Ruban AV, Horton P, Young AJ. Aggregation of higher plant xanthophylls: differences in absorption spectra and in the dependency on solvent polarity. J Photochem Photobiol B. 1993;21(2–3):229–234. https://doi.org/10.1016/1011-1344(93)80188-F
73. Barton CV, North PR. Remote sensing of canopy light use efficiency using the photochemical reflectance index. Remote Sens Environ. 2001;78(3):264–273. https://doi.org/10.1016/S0034-4257(01)00224-3
74. Plummer S. Perspectives on combining ecological process models and remotely sensed data. Ecol Modell. 2000;129(2–3):169–186. https://doi.org/10.1016/S0304-3800(00)00233-7
75. Adams III WW, Demmig-Adams B, Logan BA, Barker DH, Osmond CB. Rapid changes in xanthophyll cycle-dependent energy dissipation and photosystem II efficiency in two vines, *Stephania japonica* and *Smilax australis*, growing in the understory of an open eucalyptus forest. Plant Cell Environ. 1999;22(2):125–136. https://doi.org/10.1046/j.1365-3040.1999.00369.x
76. Lichtenthaler HK, Wellburn RR. Determination of total caretonoids and chlorophyll *a* and *b* in the leaf extracts in different solvents. Biochem Soc Trans. 1983;603:591–592. https://doi.org/10.1042/bst0110591
77. Datt B. Recognition of eucalyptus forest species using hyperspectral reflectance data. In: Stein TI, editor. IGARSS 2000. IEEE 2000 International Geoscience and Remote Sensing Symposium. Taking the pulse of the planet: the role of remote sensing in managing the environment. Proceedings (cat. No. 00CH37120); 2000 Jul 24–28; Hilton Hawaiian Village, Honolulu, Hawaii, USA. Piscataway, NJ: Institute of Electrical and Electronics Engineers; 2000. p. 1405–1407. https://doi.org/10.1109/IGARSS.2000.857221
78. Carter GA. Ratios of leaf reflectance in narrow wavebands as indicators of plant stress. Int J Remote Sens. 1994;15(3):697–703. https://doi.org/10.1080/01431169408954109
79. Cochrane MA. Spreading like wildfire – tropical forest fires in Latin America and the Caribbean: prevention, assessment and early warning. Mexico: DEWA; 2002. (Early Warning and Assessment Technical Report Series; vol 1).
80. Cochrane MA. Using vegetation reflectance variability for species level classification of hyperspectral data. Int J Remote Sens. 2000;21(10):2075–2087. https://doi.org/10.1080/01431160050021303
81. Shaw DT, Malthus TJ, Kupiec JA. High-spectral resolution data for monitoring Scots pine (*Pinus sylvestris* L.) regeneration. Int J Remote Sens. 1998;19(13):2601–2608. https://doi.org/10.1080/014311698214668
82. Cochrane MA. Synergistic Interactions between habitat fragmentation and fire in evergreen tropical forests. Conserv Biol. 2001;15(6):1515–1521. https://doi.org/10.1046/j.1523-1739.2001.01091.x